ELSEVIER

Catalysis Today 26 (1995) 283-293

CATALYSIS TODAY

# Kinetics of PdO combustion catalysis

Jon G. McCarty *

*SRI International, 333 Ravenswood Avenue, Menlo Park, CA 94025-3493, USA*

## Abstract

The kinetics of the catalytic combustion of methane by supported palladium oxide catalysts (2 wt.-% Pd/$La_2O_3 \cdot 11Al_2O_3$ and 5 wt.-% Pd/$\gamma$-$Al_2O_3$) were examined for several oxygen partial pressure levels over the temperature range from 40–900°C using temperature-programmed reaction and slow ramp and hold temperature–time transient techniques. Combustion rates were measured by differential reaction in a fixed bed of powdered catalyst at lower temperatures (200–500°C). Also, by preparing the catalysts as thin (ca. 10 $\mu$m) coatings on an alumina tube and conducting the experiments with very high flows of dilute methane and oxygen in helium, the rate measurements were extended up to 900°C without significant contribution from gas phase reactions. The specific combustion activity of supported PdO shows a persistent hysteresis between 450 and 750°C, i.e., the rate of combustion between these temperature limits depends strongly on whether the catalyst is cooling from above 750°C or heating from below 450°C. This region is also notable for negative apparent activation energy in the rate of methane oxidation, i.e., the rate increases with decreasing temperature during reoxidation of the Pd metal and decreases with increasing temperature (especially with low oxygen partial pressure) prior to decomposition of the bulk oxide. Detailed time–temperature transient kinetic analyses were performed for supported PdO catalysts within the 450–750°C temperature range. The hysteresis in methane combustion rate is caused by a higher activation energy for reduction of oxygen chemisorbed on metallic Pd and by suppressed reoxidation of Pd metal relative to PdO decomposition.

*Keywords*: Combustion; Palladium oxide combustion catalysis

## 1. Introduction

Catalytic burners for gas turbine power generation are nearing commercialization [1] in engines with moderate turbine expander inlet temperatures ( < 1250°C). The key to this technology is a catalyst that provides high steady combustion activity over the temperature range (500–900°C) without causing temperatures to exceed 1000°C [1]. Inlet stage catalysts under development for turbine combustors typically contain palladium oxide (PdO) dispersed over the surfaces of stabilized alumina supports [2,3]. The catalyst often operates at temperatures near the decomposition point of PdO, where the rate of combustion becomes nearly independent of temperature.

Supported palladium catalysts show complex behaviors for the combustion of methane over this temperature range because of the formation and decomposition of palladium oxide [3–5]. Farrauto et al. [4], examined the combustion of methane by $\gamma$-$Al_2O_3$ supported PdO over a temperature range spanning both the decomposition of PdO and the reoxidation of Pd using thermogravimetric techniques. Farrauto et al. first reported the large hysteresis in rates of methane combustion over a heating and cooling cycle and confirmed the lower rate of combustion by the metallic Pd vs. the oxide,

---

* Corresponding author.

*SSDI* 0920-5861(95)00150-6

PdO. Sekisawa et al. [5], reported a more extension examination of supported PdO using temperature programming methods similar to the current work. This authors confirmed the lower activity of metallic Pd using high temperature X-ray diffraction measurements. Although Sekisawa et al., reported that the transition to the metallic phase created a decline in activity, they did not examine the more dramatic transitions in the combustion kinetics under cooling conditions. Their results clearly show that catalytic activity for methane combustion slows or declines as the transition from PdO to the metallic phase is completed. It was not clear that the decline in catalyst activity preceded the actual decomposition of PdO as observed by Sekisawa et al., in parallel temperature programming desorption experiments.

In the present investigation, reproducible temperature and time transient kinetics of methane oxidation by PdO supported on sintered lanthanum hexa-aluminate ($La_2O_3 \cdot 11Al_2O_3$) and on $\gamma$-alumina were used to examine the phases [6] and the combustion kinetics of palladium oxides in the complex PdO/Pd/aluminate catalyst system. In particular, the time dependence of the recovery of activity in the hysteresis zone was explored to determine if the combustion activity reaches the same level if given sufficient time for transitions to occur. Experiments involving temperature-programmed reaction of methane with oxygen chemisorbed on reduced Pd and with partially decomposed PdO were performed to clearly distinguish the reactivity of different forms of oxygen.

## 2. Experimental details

### 2.1. Catalyst preparation

Commercial PdO/$\gamma$-$Al_2O_3$ (Johnson Matthey, 5 wt.-% Pd) powder and powdered and wash coated PdO catalysts (2 wt.-% Pd) supported by calcined lanthanum hexa-aluminate ($La_2O_3 \cdot 11Al_2O_3$) were used in this investigation. Calcination of the hexa-aluminate support at 1250°C for 72 h ensured that its surface area remained relatively unchanged during the course of methane combustion because the highest temperature that the catalyst reached during reaction was only 900°C. The PdO/$\gamma$-$Al_2O_3$ catalyst was only examined as a powdered bed and probed by thermal transients because it was unstable in the combustion environment at temperatures above 600°C and not suitable for repeated cycles about that temperature or for repeated cycles through the PdO/Pd transition temperature. The PdO/$La_2O_3 \cdot 11Al_2O_3$ catalyst was used in both fixed bed and wash coated annular flow reactors and examined with both time and thermal transient techniques.

For the wash coated tubular configuration, the catalyst consisted of a thin sintered layer of lanthanum hexa-aluminate ($La_2O_3 \cdot 11Al_2O_3$) oxide that was impregnated with Pd salt and dried. The first 20–25 mm of the sealed end of the 3 mm diameter alumina tube was wash coated with a finely dispersed suspension containing lanthanum hexa-aluminate. The suspension was obtained by ballmilling a mixture containing the calcined $La_2O_3 \cdot 11Al_2O_3$ powder and methyl cellulose (used as a binder) in a dilute nitric acid solution. The alumina tube was coated twice by dipping and drying then fired at 1000°C for 12 hours. The amount of $La_2O_3 \cdot 11Al_2O_3$ coated on the tube was 11.1 mg. It was then dipped into an aqueous solution of palladium(II) nitrate hydrate (Aldrich, AR grade) with required concentration ($3.4 \times 10^{-3}$ M) to give a nominal palladium loading of 2 wt.-% Pd with respect to the amount of lanthanum hexa-aluminate coating. The length of the coated section of the tube was 20 mm after removing the coatings on the tip. The catalyst was activated by heating in oxygen to 950°C before its use in measurements of the methane combustion rate.

### 2.2. Kinetic measurements with the annular reactor

Catalytic combustion of methane with oxygen diluted in helium was conducted over the $La_2O_3 \cdot 11Al_2O_3$ supported palladium catalyst.

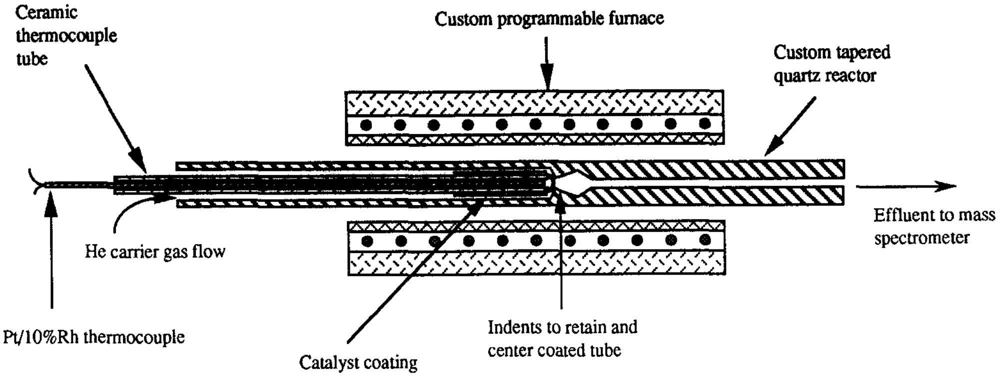

Fig. 1. Schematic drawing of the tube reactor used for high temperature kinetic rate measurements.

The thin uniform coating, the annular configuration, and the high linear velocity (2–10 m $s^{-1}$) ensured that rate measurements were possible at high temperature with minimal thermal and concentration gradients across the gas film boundary layer (Fig. 1). The methane concentration was kept constant at 0.51 vol.-%, while oxygen varied over a range of 1–41 vol.-% with helium making up the balance. Using the helium diluent and annular gap distances of 0.1–0.3 mm, analysis shows that the methane conversion under boundary layer transport limited conditions would always exceed 99%. A tapered reactor vessel was used to minimize gas phase oxidation in the downstream volume. At the point of tapering, three glass indents were used to center the catalyst coated reactor tube. The effective catalyst temperature was measured with a thermocouple probe located within the reactor tube (Fig. 1).

Kinetic experiments were conducted at total flow rates of 0.5–12 $cm^3$ $s^{-1}$ (NTP) using 5–20 mg catalyst (roughly 10–40 $\mu$m wash coat thickness). Reactor effluent compositions were analyzed by an on-line mass spectrometer. The conversion for combustion of methane was deduced from the partial pressures of the products ($CO_2$ and, rarely, CO) and the partial pressure of unconverted methane. The effective rate constants (Mols of methane converted per s per g catalyst for 1 atm of methane) reported here were calculated from the fractional conversion of methane by assuming that the reaction was first order in methane concentration. Dilute methane was used to minimize heating and to lessen the effect of product water vapor and carbon dioxide on the low temperature activity of PdO. Methane oxidation rates typically showed integral first-order reaction behavior from 300–800°C for conversions below 50% as demonstrated by reproducible, reversible, linear Arrhenius plots for the effective first-order rate constants for combustion of dilute methane by other supported metal oxides (e.g., $Mn_3O_4$).

### 2.3. Temperature-programmed experiments

Temperature-programmed desorption (TPD) experiments were conducted with the powdered catalysts and the coated tube in pure helium and in dilute oxygen (typically 1–2 vol.-% $O_2$ in He) following a variety of treatment conditions. Temperature-programmed oxidation (TPO) was conducted by cooling in dilute oxygen or by heating in dilute oxygen after a sample was first cooled to room temperature in pure helium. Temperature-programmed reaction (TPR) experiments were conducted by heating preconditioned (oxidized or decomposed) catalysts in dilute methane (typically 1.0 vol.-% $CH_4$ in He) starting from room temperature after a period of flushing in pure helium. The temperature-programmed experiments used very low gas flow rates (as low as 0.167 $cm^3/s$) to increase the sensitivity of the on-line mass spectrometric analysis. These experiments were used to investigate differences in the reactivity of oxygen present in the catalyst following various pretreatment conditions, e.g., partial decomposition, chemisorption following complete reduction, partial reoxidation, etc. Following complete reduction of the palladium oxides, typically ≤250°C, methane decomposition was always observed and identified by substantial evolution of $H_2$.

## 3. Results

### 3.1. Oxygen adsorption and desorption

The temperature-programmed decomposition (TPD) to 800°C in pure helium of a fully oxidized commercial (Johnson Matthey, 5 wt.-% Pd/alumina) PdO catalyst, and subsequent temperature-programmed reoxidation (TPO) in 0.01 atm oxygen (balance helium to 1 atm) shows a large gap (Fig. 2) between the decomposition temperature and the temperature of onset of reoxidation. This hysteresis gap was first reported by Farrauto et al. [4] using thermogravimetric analysis. The initial decomposition of the PdO precisely follows the thermodynamically equilibrium oxygen partial pressure of PdO/Pd [7,8]. Very similar TPD and TPO results are seen for our 2 wt.-% Pd/$La_2O_3 \cdot 11Al_2O_3$ catalyst. The hysteresis between oxide decomposition and reoxidation of the Pd metal gives rise to unusual kinetics in the catalytic oxidation of methane.

TPD experiments with $\gamma$-$Al_2O_3$-supported PdO (5 wt.-% Pd) consistently show two states of oxide (Fig. 3), one (often the larger) with decomposition temperatures characteristic of bulk PdO and another more stable oxide, presumably a surface or near surface oxide complex. The most volatile oxide (PdO) is more completely populated at lower temperature (350°C in Fig. 3) although oxygen uptake by the catalyst at higher temperature (550°C in Fig. 3) always populates some PdO while fully populating the higher temperature (TPD) form of oxygen. Oxygen exposure to fully reduced Pd/$\gamma$-$Al_2O_3$ apparently populates some PdO and some of the complex (TPD shows the characteristics of PdO and the higher temperature state, see Fig. 4).

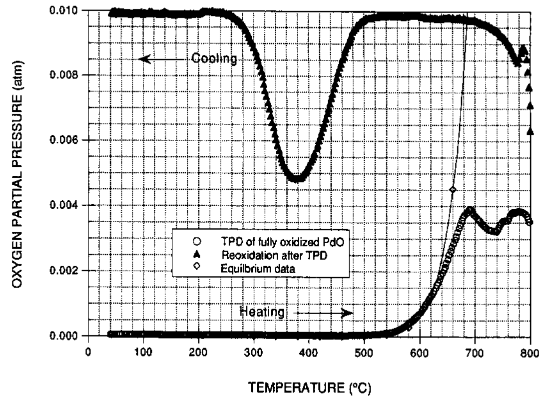

Fig. 2. Temperature programmed decomposition (heating) of a fully oxidized commercial (Johnson Matthey, 5 wt.-% Pd/$\gamma$-alumina) PdO catalyst in pure helium, followed by temperature programmed reoxidation (cooling) in 0.01 atm oxygen (balance helium) in a cooling cycle. The heating and cooling rates were 0.5°C $s^{-1}$. The decomposition and reoxidation conditions were: 123 mg catalyst; total flow rate: 50 $cm^3$ $min^{-1}$. Equilibrium data taken from Ref. [8].

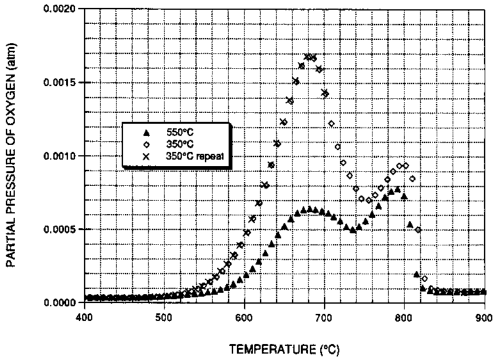

Fig. 3. Temperature-programmed decomposition with $O_2$ evolution for 5 wt.-% Pd/$\gamma$-alumina after 300 s oxidation in 0.01 atm $O_2$ at 550°C and 350°C following cooling from 800°C. The heating rates were 0.5°C $s^{-1}$.

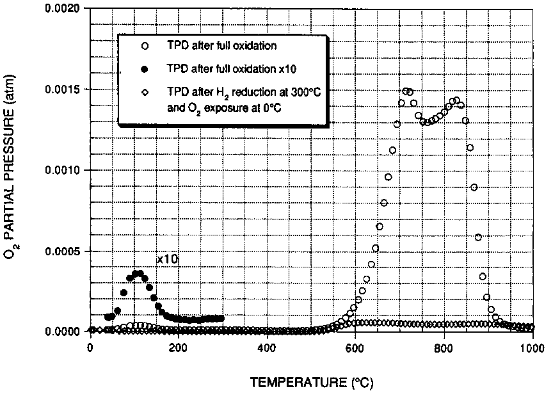

Fig. 4. Temperature-programmed decomposition of 5 wt.-% Pd/$\gamma$-alumina after full oxidation (600 s oxidation in 0.01 atm $O_2$ at 350°C) and after reduction in 0.01 atm $H_2$ at 300°C followed by $O_2$ adsorption at 0°C.

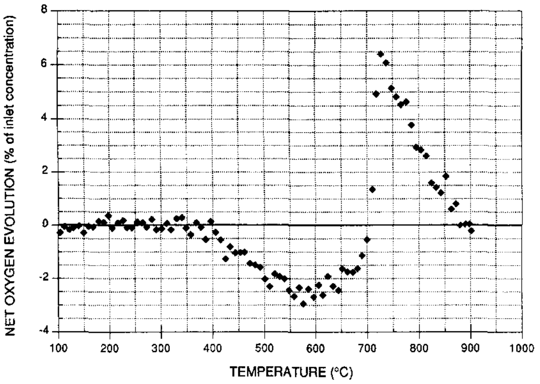

Fig. 5. TPD of the 2 wt.-% Pd/$La_2O_3 \cdot 11Al_2O_3$ catalyst (tube) in 0.02 atm $O_2$ after cooling in 0.01 atm $O_2$ from 800°C.

TPD in 0.01 atm $O_2$ with the coated tube shows oxygen uptake followed by delayed but rapidly rising desorption (Fig. 5) at 700°C. The shift in the desorption temperature is consistent with thermodynamics of the PdO/Pd system. The net uptake just prior to decomposition may reflect completion of the oxidation of underlying Pd crystallites caused by increased mobility of oxygen in the PdO lattice at the higher temperatures. The amount of oxygen released during PdO decomposition did not exceed the stoichiometric amounts (Table 1) and includes the amount absorbed during TPD just prior to reaching the decomposition temperature.

### 3.2. Reaction kinetics

Arrhenius plots of the first-order methane combustion kinetics over the 2 wt.-% Pd/$La_2O_3 \cdot 11Al_2O_3$ catalyst shows several unusual and reproducible phenomena (Fig. 6) during repeated cooling and heating cycles. During the heating ramp, the effective first-order rate constant increases with temperature to 550°C. It then shows negative apparent activation energy by *decreasing* with *increasing* temperature before showing normal Arrhenius behavior above 700°C. The deactivation of $PdO/La_2O_3 \cdot 11Al_2O_3$ occurs before the decomposition of PdO in 0.01 atm and parallel TPD/TPO experiments show that it may start to occur before decomposition and even while there is a net uptake of oxygen by the catalyst. In separate experiments with flowing oxygen (in the absence of methane) decomposition always occurred at the equilibrium point although often a net uptake of oxygen was observed between 25–150°C below the decomposition point. During the cooling ramp, the rate constant decreases with temperature, reaching a minimum at about 560°C before it *increases* with *decreasing* temperature, reaching a maximum at 417°C.

Clearly, there is a hysteresis gap in combustion rates over the temperature range, 420–680°C, just below the decomposition temperature of the PdO/Pd system. Outside this temperature range, the rate constants of the heating and cooling runs are

Table 1
Effect of composition of atmosphere on the decomposition of $PdO_x$/$La_2O_3 \cdot 11Al_2O_3$ (2 wt.-% Pd). The Pd oxides formed during treatment with ramp down from 900–40°C at a cooling rate of 30°C $min^{-1}$ in 2% $O_2$ (10 $cm^3$ $min^{-1}$)

| Atmosphere ($O_2$%) | Decomposition of $PdO_x$ | | Oxygen desorbed[c] (μmol $g^{-1}$) |
|---|---|---|---|
| | $T_{init}$ (°C)[a] | $T_{max}$ (°C)[b] | |
| 0 | 450 | 600 | 37.8 |
| 1 | 660 | 700 | 70.3 |
| 2 | 700 | 730 | 77.5 |

[a] Temperature corresponding to the start of decomposition of $PdO_x$ in TPO/TPD from 40°C to 900°C at a heating rate of 30°C $min^{-1}$.
[b] Temperature at which maximal decomposition of $PdO_x$ occurred in TPO/TPD from 40°C to 900°C at a heating rate of 30°C $min^{-1}$.
[c] As $O_2$ determined from TPO/TPD experiments. Amount of $O_2$ in PdO: 102 μmol $g^{-1}$.

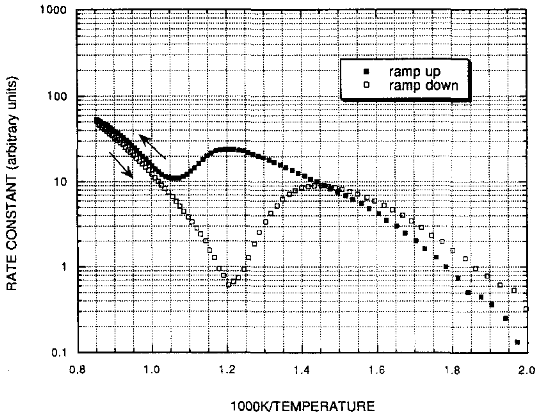

Fig. 6. Effective first order rate constant as a function of reciprocal temperatures for a methane (0.005 atm) oxidation (0.01 atm $O_2$) cooling and heating cycles over the 2 wt.-% Pd/$La_2O_3 \cdot 11Al_2O_3$ catalyst.

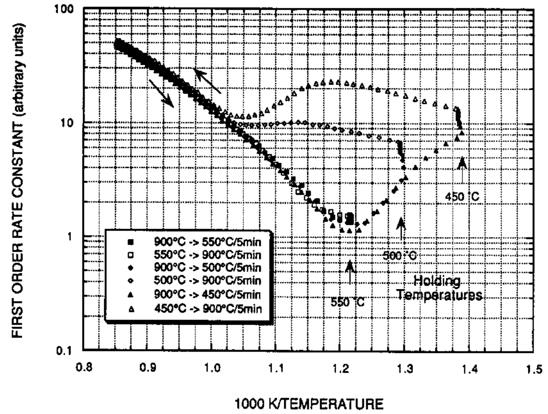

Fig. 7. Effective first order rate constant for methane oxidation over 2 wt.-% Pd/$La_2O_3 \cdot 11Al_2O_3$ catalyst-coated tube during several cooling and reheating cycles with 0.01 atm oxygen. The cooling rates were 0.5°C $s^{-1}$ to the specified temperature followed by 300 s at that temperature and reheating 0.5°C $s^{-1}$ to 900°C. The reaction conditions were: 11 mg catalyst on a 3 mm alumina tube; 0.0052 atm $CH_4$, 0.01 atm $O_2$, balance He (inlet composition); and 12.3 $cm^3$ $s^{-1}$ (NTP) gas flow rate.

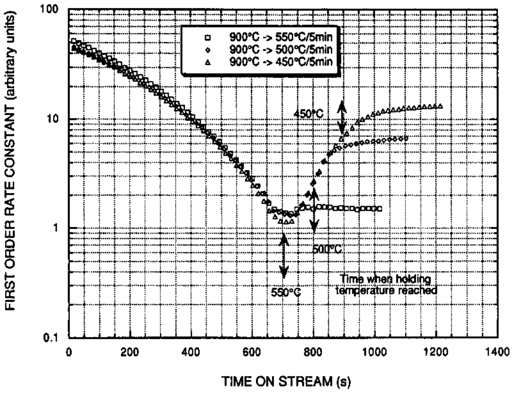

Fig. 8. Effective first order rate constant for methane oxidation vs. time for cooling cycles of Fig. 7.

reproducible and reversible. The slope of the high temperature region (Pd metal) is greater than the low temperature region (PdO) indicating that the supported bulk Pd metal has a higher activation energy for catalytic methane combustion than supported PdO. The transition region is of great interest because it contains information about the dynamics of PdO growth, sintering, and decomposition.

We used ramp and hold heating and cooling cycles to further examine the effect on the combustion kinetics of PdO formation and decomposition dynamics across the transition region (Fig. 7, Fig. 8, Fig. 9). Leaving the system at 550°C for 10 min formed only small amounts of PdO, since when the catalyst was again heated the nearly the same rate constant curve was obtained as during cooling of the supported Pd metal. During the holding period for temperatures between 550 and 450°C, the rate slowly increased with time (Fig. 8). Reheating immediately showed normal Arrhenius behavior, but a region of negative activation energy appeared (although less pronounced for higher oxygen levels) until the metallic phase formed. In similar experiments with continued cooling following holding intervals in the transition range (Fig. 9), the apparent activation energy quickly reversed from positive to negative after additional cooling of less than 25°C. Holding at 500°C for 10 min led to significant formation of PdO, but was not sufficient to fully oxidize all the Pd metal because its combustion activity is much lower than that of PdO formed by fully oxidizing the metal. Holding at 450°C for 10 min results in complete oxidation of all the Pd available, since the rate constant vs. reciprocal temperature curve falls exactly on the same curve as the fully oxidized catalyst. Thus, the development of active PdO surface is significantly temperature dependent as well as time dependent.

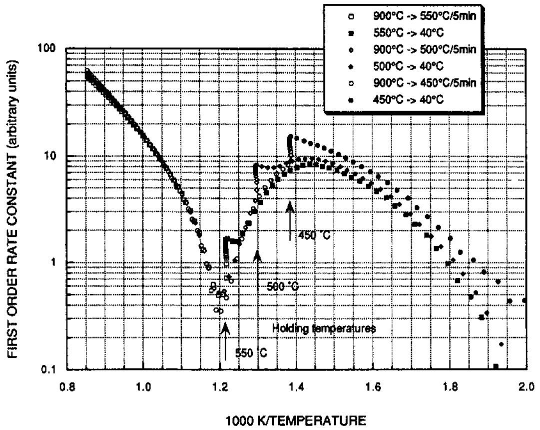

Fig. 9. Effective first-order rate constant for methane oxidation in 0.01 atm $O_2$ over the 2 wt.-% Pd/$La_2O_3 \cdot 11Al_2O_3$ catalyst-coated tube during several cooling/hold/cooling intervals. The cooling internal began at 900°C with a cooling rate of 0.5°C $s^{-1}$ to the specified temperature followed by a holding period of 300 s. Then catalyst was cooled at 0.5°C $s^{-1}$ to room temperature. Reaction conditions were as indicated in Fig. 7.

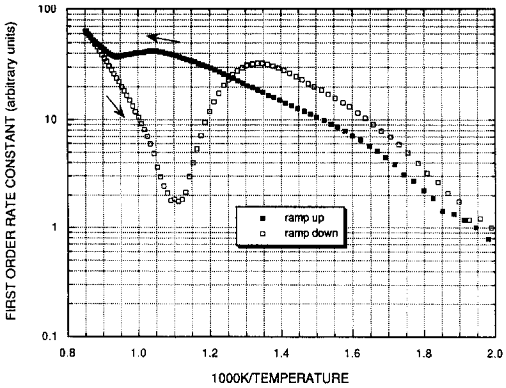

Fig. 10. Effective first-order rate constant for methane oxidation of the 2 wt.-% Pd/$La_2O_3 \cdot 11Al_2O_3$ catalyst with 0.101 atm oxygen. Cooling from 900–40°C at 0.5°C $s^{-1}$ was followed by heating from 40–900°C at the same rate. Other reaction conditions were as in Fig. 7.

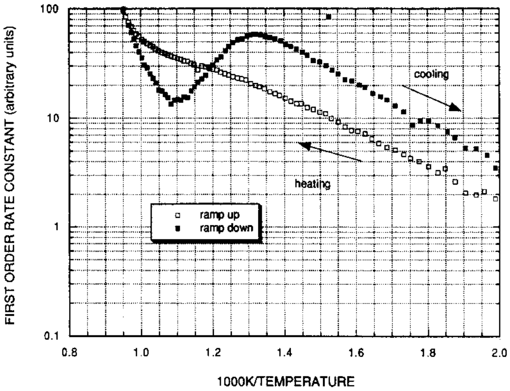

Fig. 11. Effective first order rate constant for methane oxidation of the 2 wt.-% Pd/$La_2O_3 \cdot 11Al_2O_3$ catalyst with 0.415 atm oxygen. Cooling from 900–40°C at 0.5°C $s^{-1}$ was followed by heating from 40–900°C at the same rate. Other reaction conditions were as in Fig. 7, except 0.0031 atm $CH_4$ was used and the total flow rate was 20 $cm^3 s^{-1}$ (NTP).

Similar transient experimental results were observed for methane oxidation with 0.101 atm $O_2$ (Fig. 10) and 0.411 atm $O_2$ (Fig. 11), but the degree of negative apparent activation energy diminished, especially on the heating cycle. With 0.411 atm $O_2$, the rate of oxidation continued to increase with temperature to 900°C (Fig. 11). The cooling cycle with 0.411 atm $O_2$ shows behavior similar to the case with 1 vol.-% $O_2$. With high oxygen partial pressure (especially 41 vol.-% $O_2$), formation of a partial oxidation product (carbon monoxide) was often seen at high temperature ( > 750°C), although generally controlled by increasing flow rates and by using tapered (downstream of the tube) reactors. The CO production was attributed to homogeneous reactions in the post-catalyst region of the reactor. Table 2 summarizes the results of the temperature-programmed combustion experiments. Holding at temperature for up to 600 s during reaction always gave slowly increasing rates under conditions (temperature and oxygen partial pressure) where negative apparent activation energy was observed. Holding at low temperature and holding with high oxygen levels almost always resulted in slowly decreasing rates (Table 2).

### 3.3. *Temperature-programmed reaction with methane (TPR)*

Fully oxidized PdO generally has slightly higher rates of methane oxidation during TPR

Table 2
Kinetic phenomena during cooling and heating cycles for methane oxidation over 2 wt.-% Pd/$La_2O_3 \cdot 11Al_2O_3$ catalyst

| $O_2$ conc. (vol.-%) | $T^{a}_{\text{equil}}$ (°C) | $T_{\text{hold}}$ (°C) | Rate change during hold | $E^{b}_{\text{act}}$ prior to hold |
|---|---|---|---|---|
| 1 | 677 | 550 | ⇔ | ca. 0 |
| | | 500 | ⇑ | <0 |
| | | 450 | ⇑ | <0 |
| 10.1 | 723 | 550 | ⇑ | <0 |
| | | 500 | ⇔ | <0 |
| | | 450 | ⇓ | >0 |
| 41.1 | 837 | 600 | ⇓ | <0 |
| | | 550 | ⇓ | <0 |
| | | 500 | ⇓ | <0 |

[a] Equilibrium temperature estimated from literature data [7,8].

[b] For negative apparent activation energy ($E_{\text{act}} < 0$). $E_{\text{act}}$ was always > 0 after the holding period.

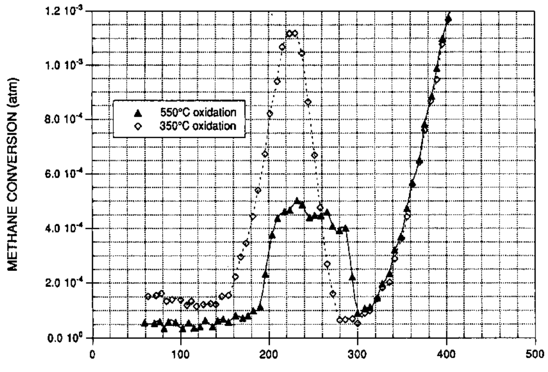

Fig. 12. Temperature-programmed reaction with 0.01 atm $CH_4$ of the 5 wt.-% Pd/γ-alumina catalyst following oxidation at 550°C and 350°C under the conditions as described in Fig. 3.

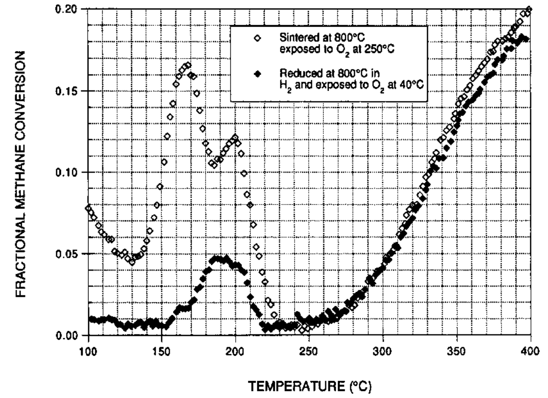

Fig. 13. Temperature-programmed reaction with 0.01 atm $CH_4$ of the 5 wt.-% Pd/γ-alumina catalyst following oxidation at 250°C and following 300 s reduction in 0.01 atm $H_2$ at 800°C, flushing 300 s in He at 800°C and oxygen adsorption at 40°C.

(temperature-programmed reaction of the oxidized catalyst with 1 vol.-% $CH_4$ and without gas phase oxygen) than partially decomposed PdO. The rates of oxidation by partially decomposed PdO are higher than fully oxidized PdO and much higher than oxygen chemisorbed on fully reduced Pd/γ-$Al_2O_3$ (Fig. 12 and Fig. 13). Catalytic oxidation of methane by γ-$Al_2O_3$-supported PdO (5 wt.-% Pd) was observed at temperatures as low as 100°C. TPR experiments show small differences (attributable to the differing amounts of oxide present) between specific methane oxidation rates with oxygen absorbed at 550°C and oxygen absorbed at 350°C (Fig. 12). Note that the condition of catalyst before the TPR curves of Fig. 12 corresponds exactly to that before the TPD curves of Fig. 3.

## 4. Discussion

### *4.1. Oxidation of supported palladium catalysts*

The behavior of the alumina-supported palladium crystallites in reducing (hydrogen) and oxidizing (oxygen) atmospheres has been studied in detail by Chen and Ruckenstein [9,10] using transmission electron microscopy (TEM). In both studies, a thin film of palladium ( ~15μm) was deposited by vacuum evaporation on an electron-transparent alumina film approximately 300 μm in thickness. In 1 atm oxygen at temperatures < 850°C, PdO crystallites formed and were found to spread over the alumina substrate. Chen and Ruckenstein [9] also found that upon heating the Pd film in pure oxygen, the crystallites of PdO that formed were not densely packed, but instead formed porous structures. They found that development of these porous structures was a function of both temperature and time. At a given temperature, the crystallites of palladium oxide became more porous as time progressed. Higher treatment temperature led to more extensive development of porous structures and eventually to the formation of cavities of different sizes. It should be noted however, that the crystallites of Chen and Ruckenstein were larger than those normally encountered in active combustion catalysts, and that the observation times (ca. $10^4$ h) were much longer than with kinetic experiments (100 s). König et al. [11], using ellipsometry, also report the growth of highly porous PdO layers 20 to 50 nm thick over 1 μm Pd films in dilute oxygen at 500°C. As in the work of Ruckenstein et al., the formation of porous oxide layers resulting from the oxidation of polycrystalline Pd films reported by König et al. may not be representative of the oxidation of individually dispersed and supported Pd metal crystallites.

Recent high resolution TEM results reported by Grabowski et al. [12], shows the slow transformation of the orientation of small Pd grains in alumina-supported catalysts, but not wetting and spreading or twinning (growth of several oxide crystals from one metal particle) or other surface enhancing transformations of the metal during its oxidation. In observations using electron diffraction with analytical TEM, we also saw that the epitaxial relationship of the freshly reduced Pd/ $\gamma$-$Al_2O_3$ catalyst as observed by these workers was lost after a single oxidation reaction reduction cycle. No evidence of growth of multiple grains from metal particles or gross irregularity in the small crystallites of either Pd or PdO was observed in our studies over our relatively short time scales. Therefore, the significant differences in methane oxidation rates and in the temperatures of desorption of oxygen for the oxide states cannot be attributed to differences in surface area, and must be considered intrinsic properties (e.g., binding energy, morphology).

The mechanism of PdO formation and decomposition on supporting oxides in a reaction stream (containing both methane and oxygen) is complex and poorly understood. Thermodynamically, PdO is stable at low temperature and high partial pressure of oxygen but oxidation of metallic supported palladium is kinetically controlled at lower temperatures and depends on crystallite size. Oxides such as $PdO_2$ and $Pd_2O_3$ are reportedly formed in electrochemistry probes of Pd electrodes, [13], but are also known to thermally decompose into PdO and $O_2$ at 200°C and 0°C, respectively [14]. Thus, the bulk palladium oxide observed at temperatures above 200°C must be PdO or some unknown suboxide. Lam and Boudart [15] showed that supported on silica supports metallic palladium will oxidize to PdO with 5–10 vol.-% of oxygen at temperatures $<260$°C. Complete oxidation of small palladium particles (ca. 70 Å) to form PdO occurred in the temperature range 265–310°C [15]. Therefore, the catalytic behavior observed in the current investigation at temperatures above 310°C is attributed to the surface layers of oxygen over Pd metal, over bulk PdO, or over bulk palladium aluminate or lanthanate ($PdO \cdot nAl_2O_3$ or $PdO \cdot nLa_2O_3$) phases.

Recent publications by several workers consistently present spectroscopic evidence (ellipsometry [11] and X-ray photoelectron spectroscopy (XPS) [12,16,17]) for oxidized Pd existing at a higher valence state than PdO following reaction in net oxidizing atmospheres. It is possible that the assignment of reference state energies and the effect of alumina combine to give the appearance of higher valence states than +2. Yet, in work on noble metal films using Raman and XPS spectroscopies, Delgas et al. [18], show that higher oxides than thermodynamically possible can be produced in surface layers over Rh metal films. This and other observations of oxide growth on noble metal surfaces lead to the conclusion that it is possible to stabilize thin (but multilayered) surface complexes of Pd metal oxide over metal crystallites.

The surface science literature reports that the heat of adsorption for chemisorbed oxygen is approximately 200 kJ/mol $O_2$ for most noble metal surfaces [19]. On the square Pd(100) surface lattice the desorption of oxygen follows a second order (atomic recombination) rate law with activation energies ranging from 230 to 120 kJ/mol $O_2$ as the coverage increases above the stable $p(2\times2)$ quarter monolayer structure [20,21]. Complex surface structures observed over Pd(100) represent a layers of distorted PdO [22,23] overlying the metal lattice. Banse and Koel [24] were able to populate complex oxides and grow oxides on Pd(111) by using $NO_2$ as the oxidizing gas. This work, using a combination of TPD and surface spectroscopies, Auger electron spectroscopy, high resolution electron loss spectroscopy and XPS, confirmed earlier reports [25] of strongly chemisorbed oxygen and also found a complex oxygen surface layer consisting of subsurface and chemisorbed oxygen and palladium oxide. Taking high probability for adsorption (ca. 0.1) reported at low coverage and the high binding energy of chemisorbed oxygen [19], desorption of oxygen should not be observed below 900°C under the TPD experiments of the current investigation. Therefore, the energy of formation of chemisorbed oxygen may be so much greater than that of the bulk oxide (220 kJ/mol $O_2$ over Pd(100) [21] and Pd(111) [24] vs. 120 kJ/mol for PdO [8]) that a full monolayer of relatively passive chemisorbed oxygen always forms over

Table 3
Reactive states of oxygen in $\gamma$-alumina-supported PdO catalysts assigned by characteristic temperatures for TPD of $O_2$ and TPR by $CH_4$

| Oxygen state[a] | Characteristic temperature | |
|---|---|---|
| | TPD(°C)[b] | TPR(°C)[c] |
| O(a)/PdO(b) | 80 | 40 |
| PdO(b) | 680 | 150–180 |
| $PdO_x$(m)/Pd(b) | 760 | 180–200 |
| O(a)/Pd(b) | >900 | ca. 200 |

[a] Key: a – chemisorbed state; m – surface complex; b – bulk phase.

[b] Temperature at which partial pressure of $O_2$ reaches 0.01 atm at a heating rate of 30°C $min^{-1}$.

[c] Temperature at which $CH_4$ conversion reaches 10% for 0.01 atm $CH_4$ at GHSV ≈ 10000 $h^{-1}$ and a heating rate of 30°C $min^{-1}$.

metallic Pd under combustion conditions inhibiting both methane reaction and oxygen absorption.

These kinetic analyses indicate that the complex catalytic behavior of supported palladium for methane oxidation over the temperature range, 400–750°C, is caused in part by the formation of a passive chemisorbed monolayer over metallic crystallites. The assignment of TPD and TPR oxygen 'states' for the current work is summarized in Table 3.

### 4.2. Activation of supported palladium oxide catalysts

Observations of differences in formation and methane combustion activity of PdO obtained from Pd by different oxidizing treatments are in general agreement with the those of many other investigators. The phenomena that activation of Pd/$\gamma$-$Al_2O_3$ catalysts occurred during the course of combustion of methane at temperatures up to 600°C were also observed by many other investigators [4,5,26–29]. The degree of activation appears more pronounced at low temperatures than at high temperatures. Baldwin and Burch [26,27] suggested that the activation was caused by restructuring of the Pd oxide crystallites. Restructuring of catalysts was also been proposed by Baddour et al. [28], in an investigation of CO oxidation over Pd/$SiO_2$ catalysts and by Hicks et al. [29], in examinations of $CH_4$ oxidation by Pd and Pt catalysts. Such kinetic studies, including the current study, cannot determine the nature of the activated oxide from measurements of relative rates. In particular, the effect of particle size and the extent of oxidation of metal particles (porous oxide film, multilayered surface complex, or oxide crystallites?) must be resolved by direct observation.

Briot and Primet [30] found that the particle size of Pd/$Al_2O_3$ freshly prepared by reduction in hydrogen was found smaller than that of Pd/$Al_2O_3$ aged at 600°C in $CH_4$ and $O_2$ streams for 14 h before reduction (70 Å compared with 150 Å, respectively). These authors concluded that the differences in combustion rates and particle morphology of bulk PdO is related to the size of the Pd crystallites (as measured after reduction).

It is clear that the activation of PdO and its deactivation by cycling and aging arise from structures not clearly identified by past and the present work. The relatively quick and extensive activation by cooling supported Pd metal under exposure to oxygen is much more rapid than heating the reduced metal in oxygen. The maximum rate seen during the cooling cycle generally exceeds the maximum rate seen for the heating cycle. The limited extent of isothermal time transients clearly show that most of the change in catalytic activity is promoted by temperature decreases and not just slow time transients. It may be that metastable surface complexes, such as $PdO_2$ or $PdO(OH)_2$, which decompose between 350 and 550°C must proceed significant oxidation of the metal. Such surface complexes may be substantially more active for methane oxidation than the surfaces of bulk PdO and certainly more active than oxygen chemisorbed on the metal. The formation of an energetic surface oxide complex may well vary depending on crystal morphology and metal grain size. The deactivation of the PdO catalyst before the transition to the metallic phase may arise from the particle size distribution of PdO crystallites and the influence of particle size on surface free energy. Temperature and oxygen partial pressure could easily play predominant roles in the extent of PdO formation, the kinetics of oxide growth, and the sintering of both metal and oxide particles.

### 4.3. Conclusions

The present transient kinetic experiments involving ramp and hold methane combustion kinetics, TPD and TPR by dilute methane of the fully oxidized, partially oxidized, and reduced PdO/$\gamma$-alumina and PdO/$La_2O_3 \cdot 11Al_2O_3$ catalysts and recent literature reports lead to a number of conclusions:

(1) the hysteresis in methane combustion activity stems from the formation a relatively stable saturated layer of chemisorbed oxygen,

(2) oxygen chemisorbed to saturation on surfaces of metallic Pd crystallites, both suppresses nucleation and growth of the active surfaces of bulk PdO and inhibits the rate of oxidation of methane,

(3) for a given oxygen partial pressure, the extent of bulk Pd reoxidation is strongly temperature (and support) dependent implying that additional free energy for nucleation or for a $PdO_x$ precursor is required for growth of high surface area PdO particles and

(4) the differences in combustion rates observed for temperatures >300°C is caused by the extent of formation of surface oxide complexes which is determined by the morphology of underlying bulk Pd metal and oxide phases which is, in turn, influenced by the thermal history of the catalyst.

## Acknowledgements

The author acknowledges the financial support of the Gas Research Institute and its industrial cosponsors and the many contributions of D.L. Lowe in catalyst preparation, V.L. Wong, Y.-F. Chang, and S. Bhatka in TPD/TPO/TPR experiments and J. McGinn of Sarnoff Laboratories in conducting the TEM examinations.

## References

[1] I. Stambler, Gas Turbine World, May-June, 1993, p. 32.
[2] R. Dalla Betta, US Patent 5 248 251 (1993).
[3] R.J. Farrauto, T. Kennelly and E.M. Waterman, US Patent 4 893 465 (1990).
[4] R.J. Farrauto, M.C. Hobson, T. Kennelly and E.M. Waterman, Appl. Catal. A: General, 81 (1992) 227.
[5] K. Sekizawa, M. Machuda, K. Eguchi and H. Arai, J. Catal., 142 (1993) 655.
[6] J.G. McCarty and Y.F. Chang, Scripta Metall. Mater., 31 (1994) 1115.
[7] W.E. Bell, R.E. Inyard and M. Tagami, J. Phys. Chem., 70 (1966) 3735.
[8] K. Kleykamp, Z. Phys. Chem. N.F., 71 (1970) 142.
[9] J.J. Chen and E. Ruckenstein, J. Phys. Chem., 85 (1981) 1606.
[10] J.J. Chen and E. Ruckenstein, J. Catal., 69 (1981) 254.
[11] D. König, W.H. Weber, B.D. Poindexter, J.R. McBride, G.W. Graham and K. Otto, Catal. Lett., 29 (1994) 329.
[12] E. Grabowski, C. Feumi-Jantou, N. Mouaddib and M. Primet, Appl. Catal. A: General, 109 (1994) 277.
[13] V. Chausse, P. Regull and L. Victori, J. Electroanal. Chem., 238 (1987) 115.
[14] G.V. Samsonov (Ed.), The Oxide Handbook, Plenum, New York, 1973, pp. 97, 217.
[15] Y.L. Lam and M. Boudart, J. Catal., 47 (1977) 393.
[16] K. Otto, L.P. Haack and J.E. de Vries, Appl. Catal. B: Environmental, 1 (1992) 1.
[17] P. Albers, K. Seibold, K. R. Thampi, M. Grätzel and J. Kiwi, J. Chem. Soc. Faraday Trans., 86 (1990) 3671.
[18] A.A. Tolia, R.J. Smiley, W.N. Delgass, C.G. Takoudis and M.J. Weaver, J. Catal., 150 (1994) 56.
[19] T. Engel and G. Ertl, Adv. Catal., 38 (1979) 1.
[20] E.M. Stuve, R.J. Madix and C.R. Brundle, Surf. Sci., 146 (1984) 155.
[21] E.M. Stuve, S.W. Jorgensen and R.J. Madix, Surf. Sci., 146 (1984) 179.
[22] S.-L. Chang, P.A. Thiel and J.W. Evans, Surf. Sci., 205 (1988) 117.
[23] D.T. Vu, K.A.R. Mitchell, O.L. Warren and P.A. Thiel, Surf. Sci., 318 (1994) 129.
[24] B.A. Banse and B.E. Koel, Surf. Sci., 232 (1990) 275.
[25] H. Weissman, Surf. Sci., 92 (1980) L59.
[26] T.R. Baldwin and R. Burch, Appl. Catal., 66 (1990) 337.
[27] T.R. Baldwin and R. Burch, Appl. Catal., 66 (1990) 359.
[28] R.F. Baddour, M. Modell and R.L. Goldsmith, J. Phys. Chem., 74 (1970) 1787.
[29] R.F. Hicks, H. Qi, M.L. Young and R.G. Lee, J. Catal., 122 (1990) 280.
[30] P. Briot and M. Primet, Appl. Catal., 68 (1991) 301.